Laser and Particle Beams (2010), *28*, 393–397.
© Cambridge University Press, 2010 0263-0346/10 $20.00
doi:10.1017/S0263034610000376

Micro-radiography with laser plasma X-ray source operating in air atmosphere

S.A. PIKUZ, JR.,[1,2] O.V. CHEFONOV,[1] S.V. GASILOV,[1] P.S. KOMAROV,[1] A.V. OVCHINNIKOV,[1] I.YU. SKOBELEV,[1] S.YU. ASHITKOV,[1] M.V. AGRANAT,[1] A. ZIGLER,[3] AND A.YA. FAENOV[1,4]

[1]Joint Institute for High Temperatures RAS, Moscow, Russia
[2]Moscow Institute of Physics and Technology, Dolgoprudny, Russia
[3]Racah Institute of Physics, Hebrew University, Jerusalem, Israel
[4]Kansai Photon Science Institute JAEA, Kizugawa-city, Kyoto, Japan

(RECEIVED 24 February 2010; ACCEPTED 10 May 2010)

Abstract

K-shell emission from copper target was observed by focusing femtosecond laser pulses very close to the target surface-air interface. It was shown that mechanism of X-ray emission is connected with generation of fast electrons in the air plasma area. Experiments demonstrated that moderate intensity of laser radiation ($I_L < 10^{15}$ W/cm^2) was enough to produce considerable flux of X-ray photons of at least 10 keV energy. The parameters of generated X-ray emission were studied. It was found that after propagation through 40 cm thick air layer X-ray spectra consisted of pronounced K_α and K_β characteristic lines and relatively small Bremsstrahlung continuum. Since transversal source size has an order of a few tens of micrometers, such a source can be used for absorption imaging of micro-objects in standard laboratory conditions. That can be particularly important for diagnostic of medical and biological samples *in vivo*.

Keywords: Laser-produced plasma; Micro-radiography

INTRODUCTION

Development of nondestructive diagnostic techniques for study of low-contrast micro-objects is of particular importance for materials science, medicine, and high energy density physics, as well as for a number of physical and technological applications. X-ray radiography imaging is a universal technique, which allows to study objects with completely different chemical composition and spatial dimensions. Radiography techniques are extensively used for determination of internal structure of different objects using conventional two-dimensional absorption imaging, promising phase-contrast imaging, or tomography techniques (Toth *et al.*, 2007). These days, sources are developed to cover entire X-ray spectral range. Study of massive objects demands application of hard X-ray radiation ($E > 15$ keV), while X-ray-ultraviolet and soft X-ray radiation is better suited for diagnostics of submicron thick objects (Calegari *et al.*, 2007). Naturally, X-rays of intermediate energies ($E \sim 5-12$ keV) can be effectively used for the study of millimeter and submillimeter scale samples (Martz *et al.*, 2007). Apart from synchrotrons, compact imaging devices based on conventional anode tubes or microfocus tubes (Wilkins *et al.*, 1996) are being used for imaging in this spectral range. Even though X-rays in the 8–10 keV spectral regions can be used for radiography in the air atmosphere, microfocus X-ray tubes intrinsically require ultrahigh vacuum chamber in order to accelerate electron beam. At the same time another potential medium for generation of X-rays and acceleration of particle exists, namely ultrafast laser plasma. Depending on laser type and target, X-ray photons were observed in wide spectral range (Fukuda *et al.*, 2004, 2008; Hong *et al.*, 2009; Ewald *et al.*, 2002; Jiang *et al.*, 2003; Zhavoronkov *et al.*, 2005; Chakera *et al.*, 2008) as well as electrons and ions accelerated to considerable energies (Repsilber *et al.*, 2005, Roth *et al.*, 2006, Faenov *et al.*, 2007, Láska *et al.*, 2009).

The plasma emittance grows upon the increase of electron temperature and density. In order to get an effective X-ray source, it is necessary to create very dense plasma. That is why usually ultrashort intense laser pulses are focused onto the solid targets in vacuum, where the absence of gas atmosphere allows focusing laser beam in to focal spot of several wavelength diameters and to reach 10^{17}–10^{19} W/cm^2 laser

Address correspondence and reprint requests to: Anatoly Ya. Faenov, Joint Institute for High Temperatures of Russian Academy of Sciences, Izhorskaya str. 13-2, 125412 Moscow, Russia. E-mail: anatolyf@hotmail.com

https://doi.org/10.1017/S0263034610000376 Published online by Cambridge University Press

intensities. While this approach allows obtaining very bright (almost point) sources of soft and hard X-rays, it demands relatively high laser energy of several mJ and a vacuum device supplement.

Recent experiments (Hou *et al.*, 2008, Fourment *et al.*, 2009; Gordienko *et al.*, 2007) demonstrate that the interaction of short intense laser pulses with a target can lead to generation of X-ray radiation even when a target is situated in room atmosphere. However the process of laser propagation and focalization in ambient gas and following X-ray generation becomes quite more complicated. The use of micro objective allows creating the plasma area in air very close to solid target surface. In this case, at least some part of the laser radiation is able to penetrate through air plasma, which is enough to create dense hot plasma at solid target surface as a source of X-rays. At the same time, air plasma itself can be considered as a source of fast electrons providing another mechanism of X-ray photon generation at solid target surface. Due to the second mechanism, it can be expected that X-ray source of characteristic radiation will be provide by laser intensity below 10^{15} W/cm^2

This way, the more compact and convenient X-ray source can be provided for radiography applications operated in air conditions employing just femtosecond laser pulses of the 0.1 mJ energy level. Other advantages of this air based radiography source are the rapid and trouble-free setup of the investigated object, debris free operation, as well as the ability to study a living sample or species existing in a water solution.

The purpose of this work was to study the following points: (1) what is the mechanism of X-ray generation during the interaction of ultrafast ultraintense laser pulses with the solid targets in air atmosphere and (2) can such X-ray source be applied to the table top radiography of the millimeter and submillimeter scale objects in standard laboratory conditions, supposing that plasma is driven by ordinary femtosecond laser system.

EXPERIMENTAL SETUP AND DIAGNOSTIC TECHNIQUES

Experimental scheme is shown in Figure 1. Ti:Sapphire laser consisting of oscillator and single amplification stage produced 40 fs pulses with maximum energy of 600 μJ at 1 kHz repetition rate. No additional devices for enhancement of contrast were used so that laser pulses of the basic frequency ($\lambda = 1064$ nm) had contrast of 10^3 at the main pulse pedestal, 10^6 in the picosecond scale prepulse, and 10^3 with respect to nanosecond prepulse. The temporal profile of the pulse was measured by a third-order autocorrelator. Laser beam of 12 mm diameter was focused by microfocus objective with NA = 0.4 at the target surface with incidence angle of 45°. Cylinder-shape copper target was polished to ~1 μm roughness before each experiment and continuously rotated and shifted during the experiment. Laser energy was controlled by calibrated photodiode.

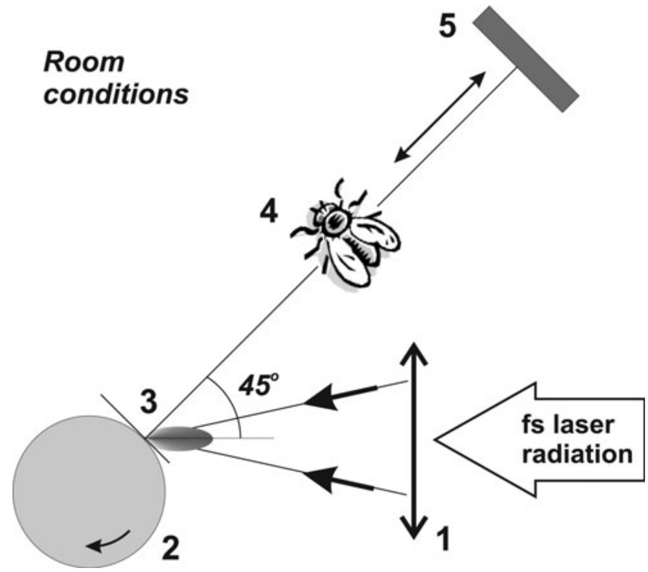

Fig. 1. Sketch of the experimental setup: **1** – microobjective, **2** – rotated and shifted bulk copper cylindrical target, **3** – air plasma induced by focused laser pulses, **4** – test or investigated object, **5** – X-ray detector (CCD).

Intensity distribution in the focal spot was measured for the laser energy below ionization threshold in air. It had Gaussian shape with the 3 μm diameter at the $1/e$ intensity level. Experiments were carried out with laser energies below 100 μJ, so that the maximum intensity in the focal spot was on the order of 10^{15} W/cm^2. The dimensions of air plasma filament were measured by imaging system and found to be 10 μm in the direction transversal to the laser pulse axis and of 100 μm in the longitudinal direction.

The creation of laser plasma in air was studied in dynamics experimentally and theoretically for 10^{14} -10^{15} W/cm^2 (Koga *et al.*, 2010) and ~10^{16} W/cm^2 (Bukin *et al.*, 2006) femtosecond laser intensities. Three stages of air laser microplasma formation were emphasized. Initially, the laser pulse ionizes the air and creates relatively cold plasma. It is resulted in the creation of plasma filament with transversal size corresponding to laser caustic. Then, the plasma is heated and the filament expands due to the effective laser-plasma interaction continues up to the falling front of laser pulse. Next, the plasma filament expands freely and reaches about 10 μm diameters at 1 ps after the laser pulse of 10^{16} W/cm^2 (Bukin *et al.*, 2006). This estimation corresponds exactly to the size of plasma radiation area measured in our experiments. Note that deeply ionized microplasma is created at the moment of the laser interaction with the gas matter.

For characterization of X-rays emitted by the plasma, we used back-illuminated charge couple device (CCD) detector with array size of 1300 × 1300 pixels and 20 μm pixel size. CCD was set to observe the plasma source in the direction close to the normal incidence on the target. Single photon counting regime for CCD was employed in order to measure X-ray emission spectra. Source size was measured using the penumbra effect observed in the images of test

https://doi.org/10.1017/S0263034610000376 Published online by Cambridge University Press

phantoms consisting either of parallel wires, or knife-like edge, or 30 μm pinhole.

X-RAY GENERATION

In a typical case, X-ray plasma emission is generated by two mechanisms. On the one hand, hot electrons generated in the plasma penetrate into the cold part of the target and create characteristic radiation. On the other hand, plasma itself produces X-ray emission due to transitions in multi-charged ions.

Let us consider the case where the laser is focused in air environment and the laser intensity exceeds air breakdown threshold ($I_L \sim 10^{15}$ W/cm^2). Such laser radiation will create air plasma area near the surface of the main target. This way, the overall mechanism of X-ray generation becomes more complicated and can be connected with fast electrons generated in the air plasma area.

The spectrum of generated plasma emission strongly depends on the mechanism of X-ray generation. In the first case of the very intense laser pulses, one can expect continuum Bremsstrahlung and photorecombination emissions with pronounced line spectrum, resulting from the transitions in the multi-charged ions. In the second case of the moderately intense laser pulses, the spectrum will resemble one of X-ray tubes and will consist of Bremsstrahlung continuum and characteristic lines.

First set of experiments was carried out to determine what physical mechanism is responsible for the X-ray generation. For the purpose of spectrum measurements, the exposure time was selected to assure that the CCD operates in single photon counting regime. The aperture of the camera was always protected from visible and ultraviolet light by 15 μm thick aluminum filter. Lowest energy detection threshold was further increased by setting the CCD camera at larger distance from the target. The minimum distance between the target and CCD was 20 cm, so that the detection threshold was about 2.5 keV due to ambient air absorption. Thus, Bremsstrahlung radiation, which had maximum at 3–4 keV depending on laser energy, was significantly attenuated by air. Moreover, the ratio between the Cu K_α line intensity and the continuum emission level increased dramatically.

The measured spectra obtained with 100 μJ laser pulse energy are shown in Figure 2. The target surface was renewed with the speed of 10 mm/s due to continuous target rotation. Unfortunately, the speed was not fast enough for the complete target renewal before each ongoing laser shot with 1 kHz repetition rate. So, the interaction regions of successive shots partially overlapped, which decreased average source emittance.

Sufficient characteristics of the X-ray yield were measured at 2×10^6 photons/s/sr in the K_α line and 2×10^5 photons/s/sr in the K_β line. These values correspond to the conversion efficiency of 10^{-8}. Note that in the similar experiment (Nagao *et al.*, 2004) carried out with picosecond pulses of much higher (three order of magnitude) energies, but with

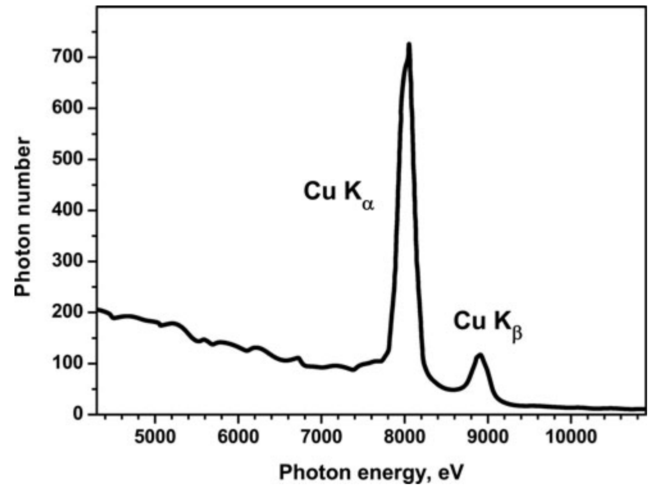

Fig. 2. X-ray spectra of the laser plasma source measured by CCD camera in single-photon-counting regime. The detection was made 30 cm from the copper target during 1 s exposure time (1000 laser shots, $E_L = 100$ μJ).

the laser intensity of about 10^{13} W/cm^2, only 3×10^3 photons/s/sr were registered.

The X-ray yield measured for different laser energies varied from 5 μJ to 100 μJ. The magnitude of the total X-ray yield, in the energy range $E > 3$ keV, had almost linear dependence on laser intensity (Fig. 3). On the other hand, X-ray yield in the K_α and K_β lines was almost negligible at below 70 μJ energy and rapidly increased above this value. It was found that the X-ray emission zone size, however, did not depend on the energy and had diameter of 60 μm measured at full width at half maximum level. Therefore, the large source size (compared with the laser focal spot or air plasma filament of 10 μm diameter) is connected with the following three occurrences: (1) the fast electrons from the air filament propagate not only in forward direction, (2) instability of the laser plasma in air, and (3) beating of the target axis changes source position.

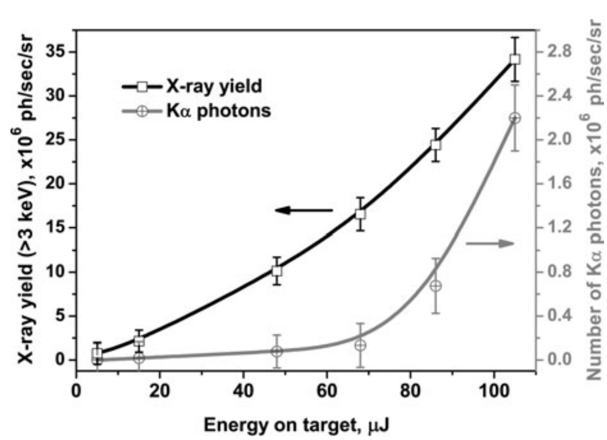

Fig. 3. Dependence of total (black) and K_α line (gray) X-ray yields on the laser pulse energy measured at the distance of 20 cm from the Copper target, irradiated by 40-fs laser pulses focused in air atmosphere.

https://doi.org/10.1017/S0263034610000376 Published online by Cambridge University Press

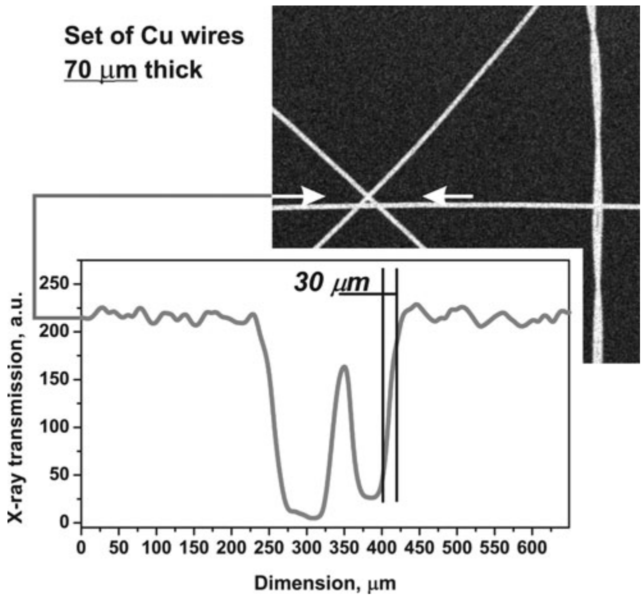

Fig. 4. X-ray shadowgraphy image of the test object (several Copper wires of 70 μm thicknesses) placed at the distance 140 mm from the source. Exposure time was 30 s. Inset shows the transmission densitogram of image fragments along the arrows.

The acquired spectra allow concluding that the mechanism of X-ray generation (at least characteristic lines from the solid target) is not connected with the target heating by laser radiation passed thought the air plasma. On the contrary, the fast electrons created inside air plasma filament interact with solid target surface and initiate characteristic X-ray radiation of the target atoms. Note that this consideration is mainly applicable for relatively low laser intensities ($I_L < 10^{15}$ W/cm^2). With the increase of laser intensity, the mechanism of direct target excitation by laser radiation will make the main impact in X-ray generation.

APPLICATION FOR RADIOGRAPHY

X-ray emission of the described air-based source was used for radiography imaging of different test objects, including micrometer thick wires, thin foils, and low contrast biological samples (see Figs. 4 and 5). Figure 4 shows shadowgraphy image of the intersection of three metal wires of 70 μm thickness that confirms the spatial resolution of 30 μm. Figure 5 contains the image of biological sample in the large field of view >2 cm^2. Here, the internal object structure is also resolved in spite of the fact that overall object thickness is only about 0.5 mm. On the inset, the trace of the insect leg image demonstrates its hollow internal structure. Also the details and features on insect wings having the thickness less than 10 μm are well distinguished that verifies the ability of the suggested imaging technique.

The increase of the laser pulse energy above the mJ level, should lead to the generation of fast electrons with up to hundred keV energies. This will allow generating more energetic photons in order to perform the diagnostics of membranes and medical samples with millimeter thicknesses. It should be noted, that using of the liquid targets in the same experimental conditions (see, for example Hatanaka *et al.*, 2008) is also very promising.

CONCLUSIONS

The approach to provide a common X-ray source for convenient radiography imaging by use of table-top femtosecond laser is successfully examined. Short laser pulse of moderate intensity $\leq 10^{15}$ W/cm^2 propagated and focused in air of room pressure causing the gas to ionize the target surface. The fast electrons of up to 10 keV energies produced in air plasma and effectively induced K-shell radiation of the copper target. The spectral distribution and geometry

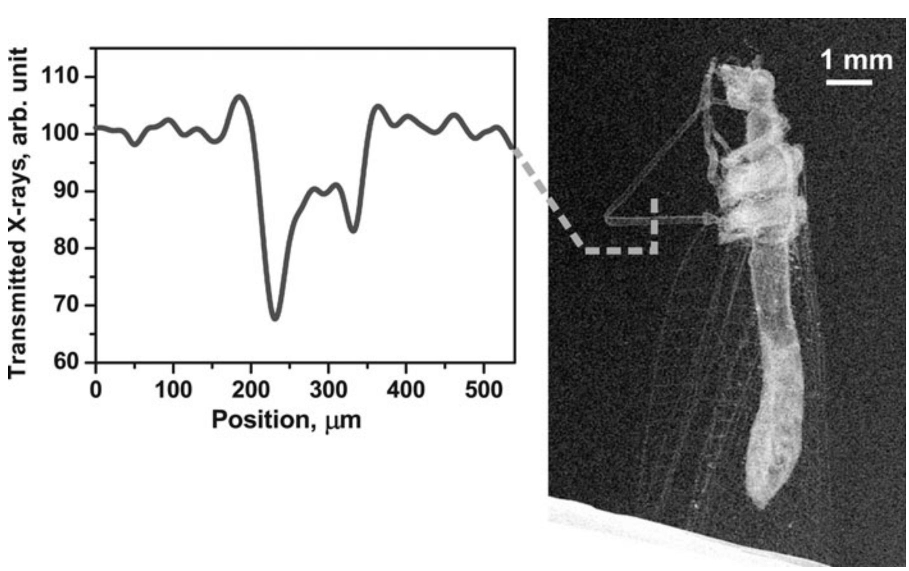

Fig. 5. X-ray shadowgraphy image of an insect obtained in the air atmosphere in 90 sec exposure time by using table-top fs-laser plasma source and Copper target. Graph inset shows intensity profile measured at the vacuum-insect leg interface.

https://doi.org/10.1017/S0263034610000376 Published online by Cambridge University Press

parameters of the source are determined. The source is experimentally proven to be applied for absorption imaging of different microstructures situated at room atmosphere environment. The advantages of the proposed method are in the smart setup of investigated object within air environment; spectral range tunability and sensitivity to weakly-absorbed or micron-thin details.

ACKNOWLEDGMENTS

This work was mutually supported by grants RFBR 09-02-92482-MNKS-a, 10-02-91174-GFEN a, 10-02-000345 a, and CRDF BRHE No. Y5-P-11-02, the Program of basic researches of Presidium RAS Nos. 12 and 27, FCP 02.740.11.0236. The work of A.Ya. Faenov was partially supported by grant No 20244065 of MEXT, Japan.

REFERENCES

Bukin, V.V., Vorob'ev, N.S., Garnov, V.I., Lozovoi, V.I., Malyutin, A.A., Shchelev, M.Ya. & Yatskovskii, I.S. (2006). Formation and development dynamics of femtosecond laser microplasma in gases. *Quan. Electron*. **36**, 638.

Calegari, F., Valentini, G., Vozzi, C., Benedetti, E., Cabanillas-Gonzalez, J., Faenov, A., Gasilov, S., Pikuz, T., Poletto, L., Sansone, G., Villoresi, P., Nisoli, M., De Silvestri, S. & Stagira, S. (2007). Elemental sensitivity in soft x-ray imaging with a laser-plasma source and a color center detector. *Opt. Lett*. **32**, 2593–2595.

Chakera, J.A., Ali, A., Tsui, Y.Y. & Fedosejevs, R. (2008). A continuous kilohertz Cu Kα source produced by submillijoule femtosecond laser pulses for phase contrast imaging. *Appl. Phys. Lett*. **93**, 261501.

Ewald, T., Schwoerer, H. & Sauerbrey, R. (2002). K_α-radiation from relativistic laser-produced plasmas. *Europhys. Lett*. **60**, 710–716.

Faenov, A.Ya., Magunov, A.I., Pikuz, T.A., Skobelev, I.Yu., Gasilov, S.V., Stagira, S., Calegari, F., Nisoli, M., De Silvestri, S., Poletto, L., Viloresi, P. & Andreev, A.A. (2007). X-ray spectroscopy observation of fast ions generation in plasma produced by short low-contrast laser pulse irradiation of solid targets. *Laser Part. Beams* **25**, 267–275.

Fourment, C., Arazam, N., Bonte, C., Caillaud, T., Descamps, D., Dorchies, F., Harmand, M., Hulin, S., Petit, S. & Santos, J.J. (2009). Broadband, high dynamics and high resolution charge coupled device-based spectrometer in dynamic mode for multi-keV repetitive x-ray sources. *Rev. Sci. Instrum*. **80**, 083505.

Fukuda, Y., Akahane, Y., Aoyama, M., Inoue, N., Ueda, H., Kishimoto, Y., Yamakawa, K., Faenov, A.Ya., Magunov, A.I., Pikuz, T.A., Skobelev, I.Yu., Abdallah, J. Jr., Csanak, G., Boldarev, A.S. & Gasilov, V.A. (2004). Generation of X rays and energetic ions from superintense laser irradiation of micron-sized Ar clusters. *Laser Part. Beams* **22**, 215–220.

Fukuda, Y., Faenov, A.Ya., Pikuz, T., Kando, M., Kotaki, H., Daito, I., Ma, J., Chen, L.M., Homma, T., Kawase, K., Kameshima, T., Kawachi, T., Daido, H., Kimura, T., Tajima, T., Kato, Y. & Bulanov, S.V. (2008). Soft X-ray source for nanostructure imaging using femtosecond-laser-irradiated clusters. *Appl. Phys. Lett*. **92**, 121110.

Gordienko, V.M., Dzhidzhoev, M.S., Zhvania, I.A. & Makarov, I.A. (2007). Increase in the yield of X-ray photons upon two-pulse laser excitation of a solid target in air. *Quan. Electron*. **37**, 599.

Hatanaka, K., Ono, H. & Fukumura, H. (2008). X-ray pulse emission from cesium chloride aqueous solutions when irradiated by double-pulsed femtosecond laser pulses. *Appl. Phys. Lett*. **93**, 064103.

Hong, W., He, Y., Wen, T., Du, H., Teng, J., Qing, X., Huang, Z., Huang, W., Liu, H., Wang, X., Huang, X., Zhu, Q., Ding, Y. & Peng, H. (2009). Spatial and temporal characteristics of X-ray emission from hot plasma driven by a relativistic femtosecond laser pulse. *Laser Part. Beams* **27**, 19–26.

Hou, B., Mordovanakis, A., Easter, J., Krushelnik, K. & Nees, J.A. (2008). Directional properties of hard x-ray sources generated by tightly focused ultrafast laser pulses. *Appl. Phys. Lett*. **93**, 201503.

Jiang, Y., Lee, T. & Rose-Petruck, C.G. (2003). Generation of ultrashort hard-x-ray pulses with tabletop laser systems at a 2-kHz repetition rate. *J. Opt. Soc. Am. B* **20**, 229–237.

Koga, J.K., Moribayashi, K., Fukuda, Y., Bulanov, S.V., Sagisaka, A., Ogura, K., Daido, H., Yamagiwa, M., Kimura, T., Fujikawa, T., Ebina, M. & Akihama, K. (2010). Simulation and experiments of the laser induced breakdown of air for femtosecond to nanosecond order pulses. *J. Phys. D*. **43**, 025204.

Láska, L., Krása, J., Velyhan, A., Jungwirth, K., Krouský, E., Margarone, D., Pfeifer, M., Rohlena, K., Ryć, L., Skála, J., Torrisi, L. & Ullschmied, J. (2009). Experimental studies of generation of ∼100 MeV Au-ions from the laser-produced plasma. *Laser Part. Beams* **27**, 137–147.

Martz Jr., H.E., Kozioziemski, B.J., Lehman, S.K., Hau-Riege, S., Schneberk, D.J. & Barty, A. (2007). Validation of radiographic simulation codes including x-ray phase effects for millimeter-size objects with micrometer structures. *J. Opt. Soc. Am. A* **24**, 169–178.

Nagao, H., Hironaka, Y., Nakamura, K.G. & Kondo, K. (2004). Hard X-ray emission from a copper target by focusing a picosecond laser beam at 3×10^{13} W/cm^2. *Jap. J. of Appl. Phys*. **43** 1207–1208.

Repsilber, T., Borghesi, M., Gauthier, J.-C., Löwenbrück, K., Mackinnon, A., Malka, V., Patel, P., Pretzler, G., Romagnani, L., Toncian, T. & Willi, O. (2005). Quantitative analysis of proton imaging measurements of laser-induced plasmas. *Appl. Phys. B* **80**, 905–913.

Roth, M., Audebert, P., Blazevic, A., Brambrink, E., Cobble, J., Cowan, T.E., Fernandez, J., Fuchs, J., Geissel, M., Hegelich, M., Karsch, S., Ruhl, H., Schollmeier, M. & Stephens, R. (2006). Laser accelerated heavy particles – Tailoring of ion beams on a nano-scale. *Opt. Comm*. **264**, 519–524.

Toth, R., Fourmaux, S., Ozaki, T., Servol, M., Kieffer, J.C., Kincaid Jr., R.E. & Krol, A. (2007). Evaluation of ultrafast laser-based hard x-ray sources for phase-contrast imaging. *Phys. plasmas* **14**, 053506.

Wilkins, S.W., Gureyev, T.E., Gao, D., Pogany, A. & Stevenson, A.W. (1996). Phase-contrast imaging using polychromatic hard X-rays. *Nat. (London)*. **384**, 335.

Zhavoronkov, N., Gritsai, Y., Bargheer, M., Woerner, M. & Elsaesser, T. (2005). Generation of ultrashort Ka radiation from quasipoint interaction area of femtosecond pulses with thin foils. *Appl. Phys. Lett*. **86**, 244107.

https://doi.org/10.1017/S0263034610000376 Published online by Cambridge University Press